

MOL #68296

Coupling to polymeric scaffolds stabilizes biofunctional peptides for intracellular applications

Ivo R. Ruttekkolk, Alokta Chakrabarti, Martin Richter, Falk Duchardt, Heike Glauner, Wouter
P. R. Verdurmen, Jörg Rademann, and Roland Brock

Department of Biochemistry, Nijmegen Centre for Molecular Life Sciences, Radboud
University Nijmegen Medical Centre, PO Box 9101, 6500 HB Nijmegen, The Netherlands
(I.R.R., A. C., W.P.R.V., F. D., H.G., R.B)

Institute of Pharmacy, Leipzig University, Brüderstraße 34, 04103 Leipzig, Germany (J.R.)
Leibniz Institute of Molecular Pharmacology (FMP), Robert-Rössle-Str. 10, 13125 Berlin,
Germany and: Institute of Chemistry and Free University Berlin, Takustr. 3, 14195 Berlin,
Germany (M.R., J.R.)

MOL #68296

Running title: Intracellular activity of polymer-coupled peptides

To whom all correspondence should be addressed:

Department of Biochemistry (286), Nijmegen Centre for Molecular Life Sciences, Radboud
University Nijmegen Medical Centre, Geert Grooteplein 28, 6525 GA Nijmegen, The
Netherlands

Ph.: +31-24-3666213

Fax: +31-24-3616413

E-mail: r.brock@ncmls.ru.nl

Text pages: 17

Tables: 1

Figures: 8

Abstract: 128 words

Introduction: 907 words

Discussion: 806 words

Number of references: 38

Abbreviations: CPP, cell-penetrating peptide; DMSO, dimethyl sulfoxide; FCS, fluorescence
correlation spectroscopy; fpm, fluorescence per molecule; HPMA, N-hydroxypropyl
methacrylamide; rfpm, relative fpm

MOL #68296

Abstract

Here, we demonstrate that coupling to N-hydroxypropyl methacrylamide (HPMA) copolymer greatly enhances the activity of apoptosis-inducing peptides inside cells. Peptides corresponding to the BH3 domain of Bid were coupled to a thioester-activated HPMA (28.5 kDa) via native chemical ligation in a simple one-pot synthesis. Peptides and polymer conjugates were introduced into cells either by electroporation or by conjugation to the cell-penetrating peptide nonaarginine. The molecular basis of the increased activity was elucidated in detail. Loading efficiency and intracellular residence time were assessed by confocal microscopy. Fluorescence correlation spectroscopy was employed as a separation-free analytical technique to determine proteolytic degradation in crude cell lysates. HPMA conjugation strongly increased the half-life of the peptides in crude cell lysates and inside cells, revealing proteolytic protection as the basis for higher activity.

MOL #68296

Introduction

The chemical nature of peptides provides a nearly infinite diversity in structure, accessible by highly robust and parallel synthesis protocols (Rademann and Jung, 2000). Therefore peptides provide a highly valuable repertoire of molecular interactors, both in basic and applied biomedical research (Cooper and Waters, 2005). In the past years, numerous peptides have been approved as drugs (Bray, 2003; Hruby and Balse, 2000; Leader et al., 2008). Nevertheless, the intracellular applicability of peptides is still limited. One major drawback of peptides is their short cytoplasmatic half-life. Major investments have been made to increase the stability of peptides. Terminal capping by acetylation (N-terminus) and amidation (C-terminus) is the most straightforward modification for increasing the resistance of a peptide to serum proteases (Brinckerhoff et al., 1999). The incorporation of non-native amino acids such as D-amino acids (Chorev et al., 1979; Tugyi et al., 2005) beta-amino acids (Frackenpohl et al., 2001; Griffith, 1986) or backbone modifications such as N-methylation (Gordon et al., 2001) have been presented as possible solutions. However, these approaches do not only render the synthesis more time-consuming and expensive, they also require a careful revalidation of the structure-activity relationship of the molecule (Ruijtenbeek et al., 2001).

An alternative approach that is well established in order to extend the plasma half-life of small molecule drugs in the bloodstream and to prevent liver accumulation is the conjugation of the drugs to high-molecular weight polymers (Duncan, 2003; Vicent and Duncan, 2006). In this context the HPMA copolymer has been widely used (Kopecek and Bazilova, 1973; Malugin et al., 2004; Satchi-Fainaro et al., 2004). For peptides, coupling to dendrimers has yielded a protection from proteolytic breakdown (Bracci et al., 2003).

In a previous study, we have shown that coupling of peptides containing an N-terminal cysteine residue to thioester-preactivated HPMA polymers is a convenient and robust method for production of polymer-coupled peptides via native chemical ligation (Dawson et al., 1994;

MOL #68296

Ruttekolk et al., 2008; Tam et al., 2001). Conjugates containing an apoptosis-enhancing peptide, loaded into cells by electroporation had a greatly increased biological activity in comparison to the free peptide. Correspondingly, bifunctional conjugates containing the apoptosis-enhancing peptide and nonaarginine (R9) as a cell-penetrating peptide (CPP) (Mitchell et al., 2000; Wender et al., 2000) showed a higher biological activity than the free bioactive peptide extended by the CPP.

Differences in import efficiency, retention time inside the cell and stabilization from proteolytic breakdown were considered as the basis for these observations. However, the structure of the bioactive peptide compromised a determination of the molecular mechanism. The peptide required free and unmodified seven N-terminal amino acids for bioactivity and could therefore only be linked to the polymer via a cysteine residue coupled to a C-terminal lysine side chain. Therefore, a fluorescence-based assessment of proteolytic cleavage of the polymer-coupled peptide was not possible. Ideally, a peptide used for the analysis of proteolytic stability should be coupled to the polymer via its N-terminus and carry a fluorescent reporter group at its C-terminus.

Here, we therefore selected a Bid-derived BH3 peptide as a model peptide (Cory et al., 2003; Kuwana et al., 2002; Willis and Adams, 2005). This peptide has a length of 22 amino acids and does not require a free amino terminus for biological activity. Coupling to the polymer occurred straightforward via an N-terminal cysteine residue. A fluorescein label was attached to a C-terminal lysine residue. Therefore, in contrast to our previous choice, this peptide was ideally suited to detect proteolytic cleavage off the polymer and release of C-terminal low molecular weight fluorescein-labeled fragments. The BH3 peptide can directly induce apoptosis by interacting with the multidomain proapoptotic BCL-2 family protein BAX. BAX forms homo-oligomers at the mitochondrial membrane and triggers the release of cytochrome c and other proapoptotic factors (Kuwana et al., 2002; Walensky et al., 2006). The induction

MOL #68296

of mitochondrial apoptosis by the Bid BH3-peptide, conjugated to the cell-penetrating peptide d-octaarginine was shown before (Goldsmith et al., 2006).

In order to eliminate the complex CPP-mediated import kinetics, involving endosomal release (Fotin-Mleczek et al., 2005), first the free peptides and the conjugates were introduced into the cell via electroporation and the bioactivity of both was investigated. The free peptide was N-terminally capped by labeling with fluorescein and C-terminally blocked by amidation. Again the polymer-coupled peptide exhibited a greatly increased activity in Jurkat T cell leukemia cells and in HeLa cells.

Import efficiency and intracellular distribution were analyzed by confocal laser scanning microscopy and flow cytometry. The intracellular retention was addressed by time-lapse microscopy in combination with quantitative image analysis. Subsequently, the proteolytic stability was compared by incubation of conjugate and peptide with crude cell lysate. The latter experiment was performed by fluorescence correlation spectroscopy (FCS) (Rigler et al., 1993). This fluorescence-based analytical technique provides information about the average number and size of fluorescently labeled molecules that diffuse through a sub-femtoliter confocal detection volume. The method is separation-free. Therefore, less than one picomole referring to a few nanograms of the labeled construct were required per measurement.

For the HPMA-peptide conjugate the import efficiency was reduced and the intracellular retention of fluorescence did not widely differ between HPMA-conjugate and free peptide. However, the stability against cytosolic proteases was tremendously increased. Finally, we demonstrate that a bifunctional HPMA-peptide conjugate, containing R9 as a cell-penetrating peptide next to the functional BH3 peptide induced apoptosis in a specific and concentration-dependent manner. Together, the results demonstrate a generalization of our HPMA-based approach and provide a mechanistic basis for the advantages of this approach.

MOL #68296

Materials and Methods

Reagents. Preactivated hydroxypropyl methacrylamide copolymer N-methacrylateglycylglycine p-nitrophenyl ester (poly-(HPMA-co-methacrylate-Gly-Gly-p-nitrophenyl ester)) with an average molecular weight (MW) of 28.5 kDa (Mw/Mn: 1.32) and a total nitrophenol content of 8.28 mol % was purchased from Polymer Laboratories (Shropshire, Great Britain). On the basis of the specifications provided by the manufacturer, 12.5 reactive groups were estimated per molecule. Peptides were purchased from EMC microcollections (Tübingen, Germany). The other chemicals for synthesis were supplied by Fluka (Deisenhofen, Germany), PD-10 columns by GE Healthcare (Uppsala, Sweden). Cell culture media were purchased from PAN biotech (Aidenbach, Germany). The electroporation kit Cell Line Nucleofector Kit V was provided by AMAXA (Cologne, Germany). Alexa647-labeled annexin-V was supplied by Invitrogen (Karlsruhe, Germany).

Peptide synthesis. Peptides were synthesized by automated solid-phase peptide synthesis using Fmoc/tBu chemistry. Fluorescein-labeled peptides with a C-terminal fluorophore were synthesized on preloaded carboxyfluorescein-labeled lysyl-Rink amide resin ((Fluo(Trt))-Lys-Rink) (Fischer et al., 2003), unlabeled peptides on Rink amide resin. N-terminal labeling proceeded as described previously (Fischer et al., 2003). The peptides were purified by preparative RP-HPLC (Grom-SIL 120 ODS-4 HE, 125× 20 mm, C18 column, 5 µm particle diameter; Grom, Herrenberg, Germany). Purity was determined by analytical RP-HPLC (Grom-SIL 120 ODS-4 HE, 100 × 2 mm, C18 column, 5 µm particle diameter; Grom), identity was validated via electrospray mass spectrometry with an LCQ Advantage Max mass spectrometer (Thermo Fisher Scientific, Waltham, USA). Concentrations were determined by

MOL #68296

UV/Vis spectroscopy of peptides and conjugates diluted 1000-fold in Tris/HCl buffer pH 8.8 assuming an extinction coefficient for fluorescein $E_{492} = 78\,000\text{ L}/(\text{mol} \times \text{cm})$.

Synthesis of HPMA-peptide conjugates. Poly(HPMA-comethacrylate-Gly-Gly-p-nitrophenylester) (4 mg) was dissolved in anhydrous benzylmercaptan (50 μL) and anhydrous dimethyl sulfoxide (DMSO; 200 μL). After 15 min, peptide was dissolved in this solution (5.6 mM corresponding to a 10-fold excess over polymer and 0.8 excess over reactive groups, respectively) and incubated for 30 min at 20 °C. After addition of thiophenol (50 μL) and incubation for 16 h at 20 °C, phosphate buffer (100 mM) and guanidinium chloride (6 M), pH 7.5 (200 μL), were added and the mixture was incubated for 72 h at 20 °C. Finally, the reaction mixture was diluted with PBS (700 μL) and purified twice with a PD-10 column followed by lyophilization. Absorption was detected at 215 nm (peptide bonds), 280 nm (aromatics), and 492 nm (fluorescein). For the bifunctional conjugates either BH3 or mBH3, and nonaarginine were conjugated to the HPMA polymer in a ratio of 10:10:1 (cargo:nonaarginine:HPMA).

Determination of stoichiometry by FCS. The determination of stoichiometry proceeded as described previously (Ruttekolk et al., 2008) using FCS. FCS measurements were performed in 384-well plates (175 μm , low-base design, MMI, Eching, Germany). A solution of 25 nM HPMA-peptide conjugate was incubated in PBS-buffer containing 40 U/mL proteinase K for 1.5 h at RT. During this incubation, autocorrelation measurements using a TCS SP5 fluorescence correlation spectroscopy equipped with an HCX PL APO 63 \times N.A. 1.2 water immersion lens (Leica Microsystems, Mannheim, Germany) were performed in regular intervals until the diffusional autocorrelation time and the amplitude of the autocorrelation function had reached a minimum. After digestion, the number of particles and the

MOL #68296

fluorescence per molecule (fpm), calculated by dividing the total background-corrected fluorescence by the number of molecules, of intact and completely digested samples were compared. The ratio of the number of particles after and before digestions represents the stoichiometry of peptides per polymer.

Electroporation. 10^6 Jurkat E6.1 cells were resuspended in 100 μ L Nucleofector Solution V (Lonza Cologne, Cologne, Germany) and the respective free peptide or HPMA-peptide conjugate was added into the electroporation cuvette (Lonza Cologne) in the desired concentration. Electroporation was performed in a Nucleofector (Lonza Cologne) using the electroporation method X-001 according to the recommendations of the manufacturer. Subsequently, 900 μ L RPMI medium was added carefully and the cells were incubated for 5 min at RT, followed by washing of the cell suspension in medium by centrifugation. HeLa cells were electroporated in a total volume of 500 μ l at a density of 10^7 cells/ml using a 10 ms pulse of 300 V (Fischer Electroporator, Heidelberg). Cells were then resuspended in fresh medium and incubated for 6 h at 37°C.

Bioactivity of conjugates. For the testing of the activity of electroporated conjugates by annexin V staining, the electroporated cells were washed, transferred to a 24-well tissue culture plate with flat bottom (Sarstedt, Nümbrecht, Germany) and incubated for 20 h in RPMI medium. Subsequently, the cells were washed in cold PBS and incubated in 100 μ L annexin-binding buffer (10 mM HEPES, 140 mM NaCl and 2.5 mM CaCl_2 , pH 7.4) containing 5 μ L annexin-V Alexa Fluor 647 for 15 min on ice. 400 μ L annexin-binding buffer was added and the samples were analyzed by flow cytometry with a FACSCalibur System (BD Biosciences, San Jose, USA).

MOL #68296

For microscopy, using an LSM510 confocal microscope (Carl Zeiss, Jena, Germany), Alexa647-labeled annexin V was excited with a 633 nm helium-neon laser and fluorescence detected using an LP 650 long pass filter.

Caspase activity was measured in HeLa and Jurkat cells electroporated with peptides or polymers as described above. Furthermore, cell-penetrating constructs were tested on Jurkat cells. 10^6 Jurkat E6.1 cells were incubated with increasing concentrations of free BH3-R9 / mBH3-R9 peptide and R9-HPMA-BH3 / R9-HPMA-mBH3 conjugates for 6 hours at 37°C. Cells were washed once with ice-cold PBS, lysed in lysis buffer (20 mM Tris/HCl, 150 mM NaCl, 1 mM EDTA, 1% Triton X-100, pH 7.7) supplemented with protease inhibitor cocktail tablets (Roche Diagnostics, Mannheim, Germany) for half an hour on ice. The protein content in lysates was determined using a commercially available Bradford protein assay kit (Bio Rad Laboratories, München, Germany). Equivalent amounts of 20 µg protein for each sample were diluted in caspase activity buffer (20 mM HEPES, 10 mM dithiothreitol, 10% glycerol, 100 mM NaCl, pH 7.5). Fluorogenic caspase-3 substrate (Ac-DEVD-AMC, Calbiochem, Bad Soden, Germany) was added to the samples to a final concentration of 2 µM. Fluorescence was detected in a Synergy 2 single-channel microplate reader (BioTek Instruments, Inc., Winooski, USA) and analyzed immediately after substrate addition and after 3 h incubation at 37°C.

Analysis of peptide release. 5×10^5 electroporated Jurkat E6.1 cells were incubated in 200 µL phenol red-free RPMI medium for 10 min at 37 °C until they had settled on the bottom of a 8-well chambered coverglass (Nunc, Rochester, USA). Subsequently, the cells were analyzed by confocal laser scanning microscopy using a Leica SP5 confocal microscope equipped with an HCX PL APO 63× N.A. 1.2 water immersion lens (Leica Microsystems, Mannheim, Germany). The cells were incubated at 37°C and 5 % CO₂ in a cell culture

MOL #68296

incubator and at certain time intervals confocal images were taken by laser scanning microscopy. The microscopy stage was housed in an incubator box maintained at 37°C.

Image analysis. For intracellular quantification of fluorescence, the confocal microscopy images were analyzed using the program ImageJ 1.41. The images were smoothed with a low pass filter and converted into a black and white mask with a threshold that was adjusted to include all cells. Adjacent cells were separated with a watershed operation. This binary mask was used for segmentation of the original image. Mean fluorescence intensity of the cells was then calculated.

Proteolytic stability in cell lysate. For preparation of HeLa cell lysate, 4×10^6 cells were harvested by treatment with trypsin and EDTA and washed with medium and PBS. For Jurkat cells, 5×10^7 cells were washed with PBS. Cells were resuspended in 1 mL PBS containing 1 % (v/v) Triton-X-100 and lysed for 45 min on ice. Subsequently, the cell membranes were removed by centrifugation (20,000 g for 20 min at 4°C). The supernatant was split into two aliquots of 500 μ L, each, into which either 2 μ M HPMA-BH3 conjugate or the free BH3 peptide were added. The concentration of the cell suspension was adjusted so that the degradation of the peptide and conjugate could be followed over several hours. The samples were incubated at 37°C. At the indicated times samples of 5 μ L were taken, mixed with 95 μ L protease inhibitor cocktail (Complete, Roche Diagnostics, Mannheim, Germany) and frozen. Finally, the frozen samples were thawed, 1000 μ L Tris buffer (100 mM Tris-HCl, pH 8.8) was added and aliquots of 50 μ L were transferred into a 384-well plate (175 μ m, low-base design, MMI). Autocorrelation measurements were performed using a TCS SP5 fluorescence correlation spectroscopy equipped with an HCX PL APO 63 \times N.A. 1.2 water immersion lens. The fractions of intact and degraded polymer or peptide were derived from two-component

MOL #68296

fits of the autocorrelation function. The diffusional autocorrelation times for the high-molecular weight component were fixed to values determined for the intact conjugate or peptide. The diffusional autocorrelation time for the low molecular weight component was fixed to the one of a fully degraded sample. After 24 h a high concentration of 800 U/mL proteinase K (160 U in 200 μ L) was added in order to validate the general sensitivity of the conjugates to protease degradation.

Peptide stability in living cells. 10^6 Jurkat E6.1 were electroporated with 30 μ M solutions of free BH3 peptide and HPMA-BH3 conjugate. The cells were washed by centrifugation (340 x g, 5 min) and incubated for 2 h at 37°C and 5 % CO₂. Subsequently, the cells were lysed by resuspension in 25 μ L PBS containing 1 % (v/v) Triton-X-100 for 45 min on ice. The cell membranes were removed by centrifugation (20,000 g for 20 min at 4°C). The supernatant was frozen at -20°C. Finally, the samples were thawed and analyzed by FCS as described above. In order to determine the autocorrelation times τ_D of the intact polymer/peptide 20 nM of the molecules were mixed with cell lysate of untreated Jurkat E6.1 cells.

Results

Synthesis and analytical characterization of HPMA-peptide conjugates. Following our previously published procedure (Ruttekolk et al., 2008), the BH3 peptide, containing an uncapped N-terminal cysteine residue was coupled to an active ester-activated HPMA polymer by native chemical ligation. A conjugate containing only fluorescein-labeled cysteine-lysyl moieties and a conjugate carrying a mutated BH3 peptide, in which three residues were replaced for alanines, were employed as negative controls. The positions of the first and second alanine exchanges correspond to conserved amino acids. These mutations had been implemented into negative controls before (Goldsmith et al., 2006). We had decided to

MOL #68296

introduce one more mutation as the double mutant had shown residual activity in preliminary experiments. For the determination of coupling efficiency the number of fluorescent particles before and after digestion of the HPMA-peptide conjugate with 40 U/mL proteinase K (2 U in 50 μ L) was determined by fluorescence correlation spectroscopy. Digestion led to a decrease of the amplitude of the autocorrelation function, corresponding to an increase in the number of fluorescent particles. The release of the fluorescent reporter group from the scaffold was also reflected by the shift in the diffusional autocorrelation. Completion of the reaction was confirmed by observing the reaction over time. The stoichiometry of peptide loading was derived from calculating the number of particles before and after digestion. On average each polymer carried two peptides (Tab. 1). Assuming a Poissonian distribution of coupling efficiency, at an average coupling ratio of 2 about 27 % of the conjugates carried only 1 peptide, 59 % of the polymers carried two or more peptides and 14 % of the polymers had remained unfunctionalized. Fluorescence correlation spectroscopy also revealed the molecular brightness per molecule (fpm – fluorescence per molecule), calculated by dividing the total background-corrected fluorescence of a sample by the number of molecules. As before, even though the polymer on average carried two fluorophores per molecule, the molecular brightness was the same for the polymers and for the free peptide (Tab. 1). This observation is very likely due to quenching of fluorescence.

Bioactivity of electroporated conjugates. Cellular import by electroporation of functional conjugates lacking a cell-penetrating moiety was chosen to elucidate whether coupling to the polymer affected the activity per peptide. In electroporation cells are briefly exposed to a strong electric field that transiently introduces pores into the plasma membrane (Gehl, 2003). Electroporation is a powerful method to introduce molecules directly into the cytoplasm of cells. For our analyses of intracellular activity, electroporation therefore circumvented the

MOL #68296

complications of endosomal uptake, breakdown and release associated with CPP-mediated cellular import (Fischer et al., 2005; Fotin-Mleczek et al., 2005). After washing by centrifugation, Jurkat E6.1 or HeLa cells were incubated for 6 h to allow the induction of apoptosis. Apoptosis induction was assessed by measuring caspase-3 activity. As a further assay for induction of apoptosis, Jurkat E6.1 cells were incubated with annexin-V Alexa fluor 647. Annexin-V binds to the phospholipid phosphatidylserine on the cell surface, which is externalized to the outer leaflet of the plasma membrane during apoptosis. An increase in caspase-3 activity was observed for the HPMA-BH3 conjugates in Jurkat E6.1 and HeLa cells (Fig. 1A-B). As the indicated concentrations represent peptide concentrations, this result demonstrates that the specific activity of the peptides was increased considerably due to the conjugation of the peptides to polymers. Annexin-V confirmed that only the HPMA-BH3 conjugate initiated apoptosis in a concentration-dependent manner, but not the mutant HPMA-mBH3 or the cysteine-containing HPMA construct (Fig. 1C-E).

We then aimed to resolve the molecular basis of the different activities. Next to a mere difference in electroporation efficiency of the polymer and the free peptide, differences in intracellular residence time or stabilization from proteolytic breakdown were considered.

Quantification of electroporation efficiency. In a first step, we compared the electroporation efficiency of the conjugates and the free peptides. To this end, 30 μ M of the free BH3 peptide and the HPMA-BH3 conjugate were electroporated into Jurkat E6.1 cells. The intracellular fluorescence was quantified by flow cytometry and observed by confocal laser scanning microscopy 1 h after electroporation. All electroporated cells were positive for fluorescence. The fluorescence of cells loaded with the free BH3 peptide was approximately 4-fold higher than that of cells loaded with the HPMA-BH3 conjugate (Fig. 2). Considering that (i) the polymer carried on average two BH3 peptides per polymer and (ii) both the free

MOL #68296

BH3 peptide and the HPMA-BH3 conjugate had the same molecular brightness, irrespective of the fact that the polymer carried on average two peptides, this finding indicated that in case of the free peptide about twice as many peptides were inside the cells than in the case of the polymer-coupled peptides.

Determination of intracellular retention. The induction of apoptosis was determined 6 and 20 h after electroporation. We therefore reasoned that the higher biological activity could be explained by a longer residence time of the higher molecular weight conjugates. For a comparison of residence times, Jurkat E6.1 cells were electroporated with 30 μ M solutions of the peptides and conjugates. The cells were washed and observed by confocal laser scanning microscopy over time in a chase experiment (Fig. 3). Subsequently, the images were analyzed by digital image analysis and the average brightness of the cells was calculated (Fig. 4). The fluorescence residence time of the unbound BH3 peptide had a half-life of 5.8 ± 1.8 h, the one for the free mBH3 peptide 5.0 ± 1.1 h, the HPMA-BH3 conjugate 10.6 ± 7.4 h and the HPMA-mBH3 conjugate 4.4 ± 1.7 h. In contrast, the free fluorescein molecules had an intracellular half-life of less than 0.5 h. For the HPMA-conjugates larger errors were found repeatedly due to the lower intensity of cellular fluorescence that also precluded an observation over longer times. The intracellular distribution did not change significantly over time (Fig. 5). In all cases, fluorescence remained homogeneously distributed inside the cytoplasm demonstrating that no sequestration into intracellular structures occurred. These results indicate that rapid cellular exit of the free peptide cannot be the reason for the increased activity of HPMA-conjugated peptides.

Peptide stability in cell lysate. Having excluded differences in loading and rapid cellular exit of the free peptide as the source for the increased biological activity, we therefore addressed

MOL #68296

the sensitivity to proteolytic breakdown of the free and the HPMA-conjugated peptide. Intracellular fluorescence may as well result from biologically inactive fragments that are retained within the cells. Therefore, the comparable intracellular residence times do not necessarily provide information on the presence of biologically active molecules. HPMA-BH3 conjugate and free BH3 peptide were incubated with crude HeLa or Jurkat E6.1 cell lysate as a source of proteolytic activity. The concentrations of the lysates were adjusted so that the degradation of peptide and conjugate could be followed over several hours. The samples were incubated at 37 °C for 24 h. At certain times aliquots were extracted. Degradation was assessed by fluorescence correlation spectroscopy. In a representative experiment the autocorrelation time τ_D for the intact HPMA-BH3 conjugate was 93 μ s, for the undigested free BH3 peptide 51 μ s and for the digested samples 35 μ s. By fixing these values, the fractions of intact and degraded polymer/peptide were derived from two component fits to the autocorrelation functions. With the selected concentration of cell lysate, the HPMA-BH3 conjugate showed a half-life of > 10 h whereas the unbound free BH3 peptide showed a half-life of only 1.1 ± 0.1 h (Fig. 6). The complete degradation of both, free peptide and conjugate upon treatment with proteinase K confirmed that both molecules could be in principle digested by proteases. The results revealed that the HPMA conjugation stabilizes the peptide from being proteolytically digested in cell lysate. Given the very similar loading efficiencies and the absence of a rapid cellular exit of the free peptide, protection from proteolytic breakdown should therefore be the explanation for the higher biological activity. This result also indicates that for the free peptide intracellular retention of fluorescence does not correlate with stability. The results suggest that proteolytic fragments are formed that are retained within the cell.

MOL #68296

Peptide stability in cells. In order to directly address differences in proteolytic degradation inside cells, Jurkat E6.1 cells were electroporated with 30 μ M solutions of free BH3 peptide and HPMA-BH3. Following a 2-h incubation at 37°C cells were lysed and cell lysates analyzed by FCS. The autocorrelation times τ_D of the intact polymer and peptide were determined by adding these molecules to cell lysates of untreated cells. In a representative experiment the τ_D for the intact HPMA-BH3 conjugate was 97 μ s, for the undigested BH3 peptide 57 μ s and for the digested samples 25 μ s. By fixing these values, the fractions of intact and degraded polymer/peptide were derived from two component fits to the autocorrelation functions. After an incubation time of 2 h the free BH3 peptide was nearly fully degraded, as only 6 % of the peptide was intact, whereas 68 % of the HPMA-BH3 was still intact (Fig. 7). As shown for cell lysate above also in living cells the HPMA conjugated peptides are more stable.

Biological activity of a bifunctional cell-penetrating conjugate. Finally, we addressed whether cofunctionalization of the HPMA polymer with a cell-penetrating moiety would yield a bioactive conjugate to induce apoptosis by CPP-mediated cell entry. The modular assembly of CPP and BH3 peptide as independent building blocks on the polymer backbone constitutes a clear advantage over the synthesis of one long cell-penetrating BH3-R9 peptide.

The conjugate effectively induced apoptosis in Jurkat cells in a concentration-dependent manner as measured by caspase-3 activation, while the conjugate functionalized with the mutated peptide did not (Fig. 8). The R9-HPMA-BH3 conjugate was more effective in inducing apoptosis than the free R9-BH3 peptide, consistent with the results for the electroporated peptides. The mutant free R9-conjugated mBH3 peptide also induced some apoptosis, albeit less reproducibly and to a lesser extent than the R9-HPMA-BH3 conjugate.

MOL #68296

Discussion

Our previous analyses had shown that coupling of peptides to an HPMA polymer by native chemical ligation yielded bioactive conjugates by a modular design (Ruttekolk et al., 2008). These initial analyses had already indicated that the polymer-coupled peptides had a higher activity per peptide moiety. Differences in cellular loading efficiency, in retention inside the cell as well as in peptide stability were considered as the molecular basis for this observation. However, the bioactive peptide, derived from the proapoptotic protein Smac (Fulda et al., 2002), that we had selected, was not accessible to an elucidation of these questions. For this peptide a free amino terminus was required for activity. Therefore, coupling to the polymer occurred via a cysteine residue coupled to a lysine side chain at the C-terminus of the peptide. Here, we selected an apoptosis-inducing peptide derived from the proapoptotic Bid protein that could be coupled to the polymer via the N-terminus in a straightforward manner. Coupling efficiencies for this longer peptide were in the same range as those reported before, confirming the general usefulness and robustness of this synthesis procedure.

Using this peptide we demonstrate an increase in the activity per peptide moiety that is very likely due to a protection from proteolytic degradation. Given the faster degradation of the free peptide one could also expect a faster release of degradation products from the cells. However, cellular retention times of fluorescence were not markedly different for the free peptides and for conjugates. We explain this observation by the generation of fluorescein-containing fragments that were still efficiently retained within the cells. We have indications from other experiments that negatively charged peptides are retained more strongly inside a cell than positively charged or neutral ones. The two N-terminal amino acid residues glutamic acid and aspartic acid are negatively charged.

For the HPMA-conjugated peptide the activity was increased considerably per peptide moiety. The HPMA-mBH3 conjugate and the fluorescein-conjugated polymer did not show

MOL #68296

any activity. This finding confirmed that induction of caspase-3 activity and phosphatidylserine exposure were not due to electroporation or to a toxic effect by the polymer itself.

In contrast to the HPMA-BH3 conjugate, the free BH3 peptide did not show any activity, in spite of the higher electroporation efficiency. For this free peptide, in vitro assays had shown that concentrations of 10 μ M and more were required to induce formation of Bax oligomers (Kuwana et al., 2005). Only for a membrane-targeted analog (Oh et al., 2006) or a peptide with a stabilized α -helix (Walensky et al., 2006) were activities at lower concentrations observed. We therefore conclude that due to the rapid proteolytic breakdown of the free peptide concentrations required for activity were not reached.

A conjugate of this peptide to the CPP d-octaarginine had shown apoptosis inducing activity in a number of cancer cells (Goldsmith et al., 2006) at concentrations of 20 μ M and higher. These concentrations were higher than the ones used for the cell-penetrating conjugate in our experiments.

While our studies focused on the intracellular pharmacokinetics of the free peptides and HPMA-peptide conjugates, it is nevertheless interesting to note that the HPMA-BH3 conjugate was active in spite of its lower electroporation efficiency. It is tempting to speculate that next to the proteolytic stabilization, the multivalency of this conjugate may contribute to this observation. This multivalency should enable the simultaneous interaction with at least two Bax molecules. In nature and also in the generation of synthetic binders, multivalency is a highly powerful principle for increasing the interaction of low-affinity binders (Lee and Lee, 2000; Rao et al., 1998).

Finally, the HPMA-based strategy also proved its potential as a modular synthesis approach for the combination of different functionalities. Synthesis of a single 31 amino acid peptide containing the BH3 domain and the nonaarginine CPP is a major challenge and we repeatedly

MOL #68296

obtained this peptide only with low purities and yields. Fusion of peptide fragments by native chemical ligation requires synthesis of a C-terminal thioester, which is also not straightforward in Fmoc peptide chemistry. Separate synthesis of the functional BH3 peptide and the CPP and incorporation into the polymer therefore constitutes a major synthetic advantage.

For the cell-penetrating R9-HPMA-BH3 conjugate the same higher activity was observed in comparison to the free peptide as was observed for the molecules that were loaded by electroporation.

In summary, our results provide a powerful methodological approach to address the pharmacokinetics of peptides and polymer conjugates in intracellular applications. Fluorescence correlation spectroscopy was employed as an analytical method to determine proteolytic degradation in microliter volumes of crude cell lysates in a separation-free manner. The analyses demonstrate that conjugation of peptides to the HPMA polymer confers significant protection from proteolytic degradation. Together with the robust, modular synthesis procedure, these results further underline the usefulness of the HPMA-based strategy to increase the functionality of peptides in intracellular applications in fundamental and applied biomedical research.

Acknowledgements

We thank Peter van Gaalen, Institute for Molecules and Materials, Radboud University Nijmegen, for the technical assistance regarding the electrospray mass spectrometry measurements. We are grateful to Dr. Michael Beyermann, FMP, for his support in peptide synthesis.

MOL #68296

Authorship contributions

Participated in research design: Ruttekolk, Rademann, Brock

Conducted experiments: Ruttekolk, Chakrabarti, Richter, Duchardt, Glauner

Performed data analysis: Ruttekolk, Chakrabarti, Verdurmen, Brock

Wrote or contributed to writing of the manuscript: Ruttekolk, Verdurmen, Rademann, Brock

MOL #68296

References

- Bracci L, Falciani C, Lelli B, Lozzi L, Runci Y, Pini A, De Montis MG, Tagliamonte A and Neri P (2003) Synthetic peptides in the form of dendrimers become resistant to protease activity. *J BiolChem* **278**: 46590-46595.
- Bray BL (2003) Large-scale manufacture of peptide therapeutics by chemical synthesis. *NatRevDrug Discov* **2**: 587-593.
- Brinckerhoff LH, Kalashnikov VV, Thompson LW, Yamshchikov GV, Pierce RA, Galavotti HS, Engelhard VH and Slingluff CL, Jr. (1999) Terminal modifications inhibit proteolytic degradation of an immunogenic mart-1(27-35) peptide: Implications for peptide vaccines. *IntJ Cancer* **83**: 326-334.
- Chorev M, Shavitz R, Goodman M, Minick S and Guillemin R (1979) Partially modified retro-inverso-enkephalinamides: Topochemical long-acting analogs in vitro and in vivo. *Science* **204**: 1210-1212.
- Cooper WJ and Waters ML (2005) Molecular recognition with designed peptides and proteins. *CurrOpinChemBiol* **9**: 627-631.
- Cory S, Huang DC and Adams JM (2003) The bcl-2 family: Roles in cell survival and oncogenesis. *Oncogene* **22**: 8590-8607.
- Dawson PE, Muir TW, Clark-Lewis I and Kent SBH (1994) Synthesis of proteins by native chemical ligation. *Science* **266**: 776-779.
- Duncan R (2003) The dawning era of polymer therapeutics. *Nat Rev Drug Discov* **2**: 347-360.
- Fischer R, Fotin-Mleczek M, Hufnagel H and Brock R (2005) Break on through to the other side - biophysics and cell biology shed light on cationic cell-penetrating peptides. *ChemBioChem* **6**: 2126-2142.
- Fischer R, Mader O, Jung G and Brock R (2003) Extending the applicability of carboxyfluorescein in solid-phase synthesis. *Bioconjug Chem* **14**: 653-660.

MOL #68296

- Fotin-Mleczek M, Fischer R and Brock R (2005) Endocytosis and cationic cell-penetrating peptides - a merger of concepts and methods. *Curr Pharm Des* **11**: 3613-3628.
- Frackenpohl J, Arvidsson PI, Schreiber JV and Seebach D (2001) The outstanding biological stability of b- and g-peptides toward proteolytic enzymes: An in vitro investigation with fifteen peptidases. *ChemBioChem* **2**: 445-455.
- Fulda S, Wick W, Weller M and Debatin KM (2002) Smac agonists sensitize for apo2l/trail- or anticancer drug-induced apoptosis and induce regression of malignant glioma in vivo. *Nat Med* **8**: 808-815.
- Gehl J (2003) Electroporation: Theory and methods, perspectives for drug delivery, gene therapy and research. *Acta Physiol Scand* **177**: 437-447.
- Goldsmith KC, Liu X, Dam V, Morgan BT, Shabbout M, Cnaan A, Letai A, Korsmeyer SJ and Hogarty MD (2006) BH3 peptidomimetics potently activate apoptosis and demonstrate single agent efficacy in neuroblastoma. *Oncogene* **25**: 4525-4533.
- Gordon DJ, Sciarretta KL and Meredith SC (2001) Inhibition of beta-amyloid(40) fibrillogenesis and disassembly of beta-amyloid(40) fibrils by short beta-amyloid congeners containing n-methyl amino acids at alternate residues. *Biochemistry* **40**: 8237-8245.
- Griffith OW (1986) Beta-amino acids: Mammalian metabolism and utility as alpha-amino acid analogues. *Annu Rev vBiochem* **55**: 855-878.
- Hruby VJ and Balse PM (2000) Conformational and topographical considerations in designing agonist peptidomimetics from peptide leads. *CurrMedChem* **7**: 945-970.
- Kopecek J and Bazilova H (1973) Poly[n-(2-hydroxypropyl)methacrylamide]. I. Radical polymerization and copolymerization. *Eur Polym J* **9**: 7-14.
- Kuwana T, Bouchier-Hayes L, Chipuk JE, Bonzon C, Sullivan BA, Green DR and Newmeyer DD (2005) BH3 domains of BH3-only proteins differentially regulate bax-mediated

MOL #68296

mitochondrial membrane permeabilization both directly and indirectly. *Mol Cell* **17**: 525-535.

Kuwana T, Mackey MR, Perkins G, Ellisman MH, Latterich M, Schneiter R, Green DR and Newmeyer DD (2002) Bid, bax, and lipids cooperate to form supramolecular openings in the outer mitochondrial membrane. *Cell* **111**: 331-342.

Leader B, Baca QJ and Golan DE (2008) Protein therapeutics: A summary and pharmacological classification. *Nat Rev Drug Discov* **7**:21-39.

Lee RT and Lee YC (2000) Affinity enhancement by multivalent lectin-carbohydrate interaction. *Glycoconj J* **17**: 543-551.

Malugin A, Kopeckova P and Kopecek J (2004) HEMA copolymer-bound doxorubicin induces apoptosis in human ovarian carcinoma cells by a Fas-independent pathway. *Mol Pharm* **1**: 174-182.

Mitchell DJ, Kim DT, Steinman L, Fathman CG and Rothbard JB (2000) Polyarginine enters cells more efficiently than other polycationic homopolymers. *J Peptide Res* **56**: 318-325.

Oh KJ, Barbuto S, Pitter K, Morash J, Walensky LD and Korsmeyer SJ (2006) A membrane-targeted bid bcl-2 homology 3 peptide is sufficient for high potency activation of bax in vitro. *J Biol Chem* **281**: 36999-37008.

Rademann J and Jung G (2000) Drug discovery - integrating combinatorial synthesis and bioassays. *Science* **287**: 1947-1948.

Rao J, Lahiri J, Isaacs L, Weis RM and Whitesides GM (1998) A trivalent system from vancomycin.D-ala-d-ala with higher affinity than avidin.Biotin. *Science* **280**: 708-711.

Rigler R, Mets Ü, Widengren J and Kask P (1993) Fluorescence correlation spectroscopy with high count rate and low background: Analysis of translational diffusion. *Eur Biophys J* **22**: 169-175.

MOL #68296

- Ruijtenbeek R, Kruijtz JAW, van de Wiel W, Fischer MJE, Flück M, Redegeld FAM, Liskamp RMJ and Nijkamp FP (2001) Peptoid-peptide hybrids that bind syk sh2 domains involved in signal transduction. *ChemBioChem* **2**: 171-179.
- Ruttekolk IR, Duchardt F, Fischer R, Wiesmuller KH, Rademann J and Brock R (2008) HPMA as a scaffold for the modular assembly of functional peptide polymers by native chemical ligation. *Bioconjug Chem* **19**: 2081-2087.
- Satchi-Fainaro R, Puder M, Davies JW, Tran HT, Sampson DA, Greene AK, Corfas G and Folkman J (2004) Targeting angiogenesis with a conjugate of hpma copolymer and tnp-470. *Nat Med* **10**: 255-261.
- Tam JP, Xu J and Eom KD (2001) Methods and strategies of peptide ligation. *Biopolymers* **60**: 194-205.
- Tugyi R, Uray K, Ivan D, Fellingner E, Perkins A and Hudecz F (2005) Partial d-amino acid substitution: Improved enzymatic stability and preserved ab recognition of a muc2 epitope peptide. *Proc Natl Acad Sci USA* **102**: 413-418.
- Vicent MJ and Duncan R (2006) Polymer conjugates: Nanosized medicines for treating cancer. *Trends Biotechnol* **24**: 39-47.
- Walensky LD, Pitter K, Morash J, Oh KJ, Barbutto S, Fisher J, Smith E, Verdine GL and Korsmeyer SJ (2006) A stapled bid bh3 helix directly binds and activates bax. *Mol Cell* **24**: 199-210.
- Wender PA, Mitchell DJ, Pattabiraman K, Pelkey ET, Steinman L and Rothbard JB (2000) The design, synthesis, and evaluation of molecules that enable or enhance cellular uptake: Peptoid molecular transporters. *Proc Natl Acad Sci* **97**: 13003-13008.
- Willis SN and Adams JM (2005) Life in the balance: How BH3-only proteins induce apoptosis. *Curr Opin Cell Biol* **17**: 617-625

MOL #68296

Footnotes

This work was supported by the Volkswagen Foundation [I/77 472]; and the Deutsche Forschungsgemeinschaft [BR2443/5-1, Graduiertenkolleg 794, RA895/4-1, SFP765, project B4].

Reprint requests should be sent to

Prof. Dr. Roland Brock

Department of Biochemistry, Nijmegen Centre for Molecular Life Sciences

Radboud University Nijmegen Medical Centre, PO Box 9101 (Route 286)

6500 HB Nijmegen, The Netherlands

MOL #68296

Figure legends

Scheme 1. Synthesis of a HPMA-BH3 conjugate. (a) DMSO (anhydrous), benzylmercaptane; (b) DMSO (anhydrous), thiophenol; (c) DMSO, thiophenol, phosphate buffer (100 mM), guanidiniumchloride (6 M, pH 7.5). Amino acids are represented in single letter code and printed in italics.

Fig. 1. Apoptosis induction by HPMA-peptide conjugates and free peptides. Jurkat or HeLa cells were electroporated with the free apoptosis-inducing BH3 peptide, the mutated mBH3 peptide or the respective polymer-conjugated peptides HPMA-BH3 and HPMA-mBH3 at the indicated concentrations. (A, B) Determination of caspase-3 activity in (A) Jurkat cells and (B) HeLa cells lysed 6 h after electroporation with free peptides and HPMA-peptide conjugates. Error bars indicate the standard deviation from two independent experiments. The concentrations relate to the number of bioactive peptides. (C-E) Apoptosis detection by annexin V staining. After electroporation, the cells were washed and incubated in FCS-containing medium for 20 h with HPMA-peptide conjugates. Subsequently, cells were stained with Alexa 647-labeled annexin V. (C) Flow cytometry histograms of Jurkat cells electroporated with various concentrations of HPMA-BH3 and stained with Alexa 647-labeled annexin-V. (D) Microscopy image of annexin-V-stained cells, electroporated with 40 μ M HPMA-BH3, 20 h after incubation. (E) Annexin-V positive cells represented as the normalized fraction of annexin-V positive cells for the indicated concentrations of the HPMA-peptide constructs. The error bar shows the standard error of three independent experiments.

MOL #68296

Fig. 2. Electroporation efficiency of free peptides and HPMA-peptide conjugates. Jurkat E6.1 cells were electroporated with (A) medium 30 μM of (B) free BH3 peptide or (C) HPMA-BH3. The concentration of conjugate relates to the number of peptide moieties. Subsequently, the living cells were washed with medium and observed by (A-C) confocal laser scanning microscopy 1 h after electroporation. The scale bar in the microscopy images represents 50 μm ; (D-E) corresponding flow cytometry histograms and (G) medians of intracellular fluorescein intensities.

Fig. 3. Release of cellular fluorescence after electroporation of free peptides and HPMA-peptide conjugates. Jurkat E6.1 cells were electroporated with 30 μM of free peptides and HPMA-peptide conjugates or fluorescein. The concentration of conjugate relates to the number of peptide moieties. Subsequently, the cells were washed twice with medium, seeded into an 8-well chambered coverglass and incubated at 37°C. In certain time intervals confocal images were taken by laser scanning microscopy. The scale bar represents 50 μm .

Fig. 4. Analysis of release kinetics. The confocal images generated by laser scanning microscopy (Fig. 3) were analyzed by quantitative image analysis. (A) Superposition of all curves (the intensity at the beginning of the experiment was set to 100 %), (B) free BH3 peptide, (C) free mBH3 peptide, (D) HPMA-BH3 conjugate, (E) HPMA-mBH3 conjugate and (F) fluorescein. The data were fitted with a first order exponential decay.

Fig. 5. Intracellular distribution of fluorescence at different time points after electroporation. Jurkat E6.1 cells electroporated with (A) the free BH3 peptide, (B) the HPMA-BH3 conjugate, (C) the free mBH3 peptide, (D) the HPMA-mBH3 conjugate and (F) fluorescein

MOL #68296

were observed (A-E) 30 min after electroporation and (F-J) 6 h after electroporation. The scale bar represents 20 μm .

Fig. 6. Proteolytic stability of HPMA-BH3 and the free BH3 peptide in crude cell lysates of (A) HeLa and (B) Jurkat E6.1 cells. Cell lysate was generated by lysis of cells in Triton-X-100. The cell lysate was mixed with 2 μM HPMA-BH3 conjugate or free BH3 peptide and the samples were incubated at 37°C. The concentration is related to the number of peptide moieties. After certain time points samples were extracted and frozen. After 24 h proteinase K was added to the samples in order to confirm the general sensitivity to proteases. The fractions of intact conjugate (filled squares) and peptide (blank circles) were determined by fluorescence correlation spectroscopy and derived from two-component fits of the autocorrelation functions. Half-lives were derived from first-order exponential fits. Each panel shows the results of a representative experiment for either cell line.

Fig. 7. Proteolytic stability of HPMA-BH3 and the free BH3 peptide in living Jurkat E6.1 cells. The conjugate/peptide was electroporated into cells. After incubation cell lysate was generated and measured by FCS. Whereas the (A) diffusion time τ_D of the free BH3 peptide decreased significantly upon incubation in cells, the (B) τ_D of the HPMA-BH3 decreased only slightly. The shifts in diffusional autocorrelation times between the intact conjugate or peptide (solid lines) and the incubated samples (dashed lines) are indicated by arrows.

Fig. 8. Apoptosis induction by R9-HPMA-BH3. Jurkat cells were incubated with conjugates for 6 h at 37 °C. Titration of cells with HPMA-R9 conjugates and peptide-R9 conjugates and determination of caspase-3-activity. Concentrations of the polymer conjugates in the medium were adjusted to the same concentration with respect to the functional peptide. For the HPMA

MOL #68296

conjugates and the free peptides, the normalized mean and mean error of two and four independent experiments is shown.

MOL #68296

Tab. 1. Peptides and HPMA conjugates.

name	conjugate	fold excess	fluo- analog per polymer ¹	reactive groups coupled to fluo- analog	Rfpm ²
BH3	Fluo-EDIIRNIARHLAQVGDSDRSI	/	/	/	/
mBH3	Fluo-EDIIRNIARH <u>AA</u> QV <u>GA</u> S <u>AD</u> RSI ³	/	/	/	/
BH3-R9	Fluo-EDIIRNIARHLAQVGDSDRSI-R9	/	/	/	/
mBH3-R9	Fluo-EDIIRNIARH <u>AA</u> QV <u>GA</u> S <u>AD</u> RSI-R9 ³	/	/	/	/
HPMA-BH3	HPMA-CEDIIRNIARHLAQVGDSDRSI(Fluo)	10:1	1.8	14%	1.2
HPMA-mBH3	HPMA-CEDIIRNIARH <u>AA</u> QV <u>GA</u> S <u>AD</u> RSI(Fluo) ³	10:1	2.1	17%	1.0
R9-HPMA-BH3	R9-HPMA-CEDIIRNIARHLAQVGDSDRSI(Fluo)	10:10:1	2.4	19%	1.2
R9-HPMA-mBH3	R9-HPMA-CEDIIRNIARH <u>AA</u> QV <u>GA</u> S <u>AD</u> RSI(Fluo) ³	10:10:1	2.8	22%	1.1

¹The loading refers to the fluorescein moieties per polymer.

²the relative fluorescence per molecule (rfpm) was determined by dividing the fluorescence per molecule for the conjugate through the one of the released peptide. The fpm were determined by FCS

³The mutated amino acid residues are underlined.

Scheme 1

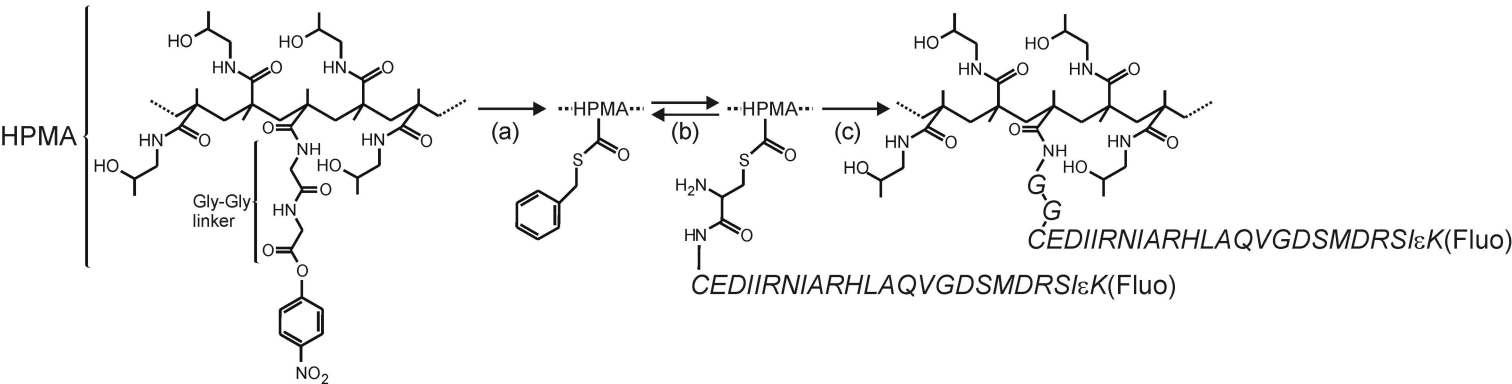


Figure 1

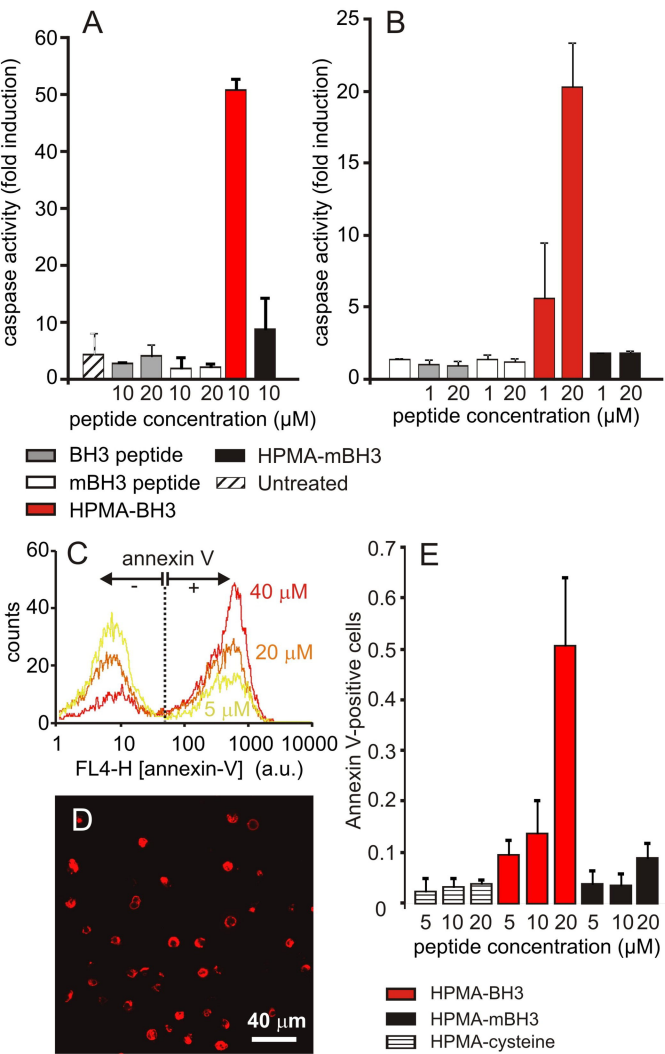


Figure 2

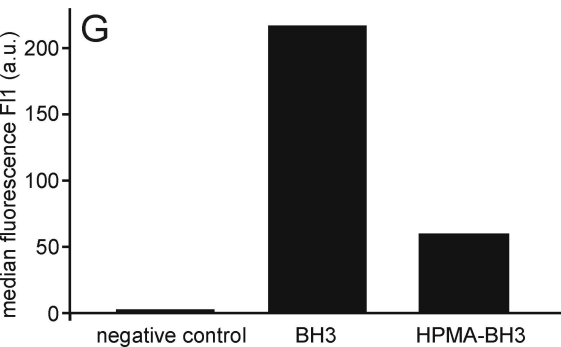
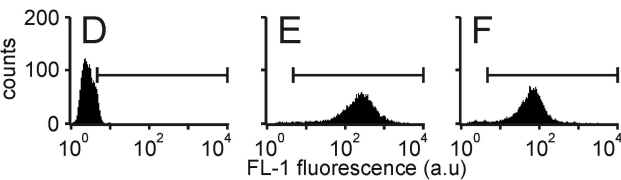
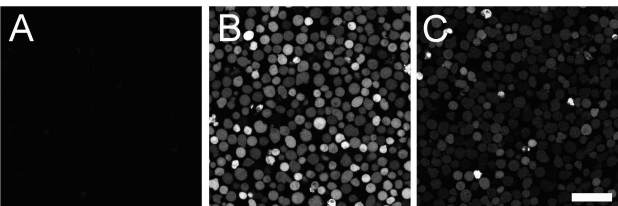


Figure 3

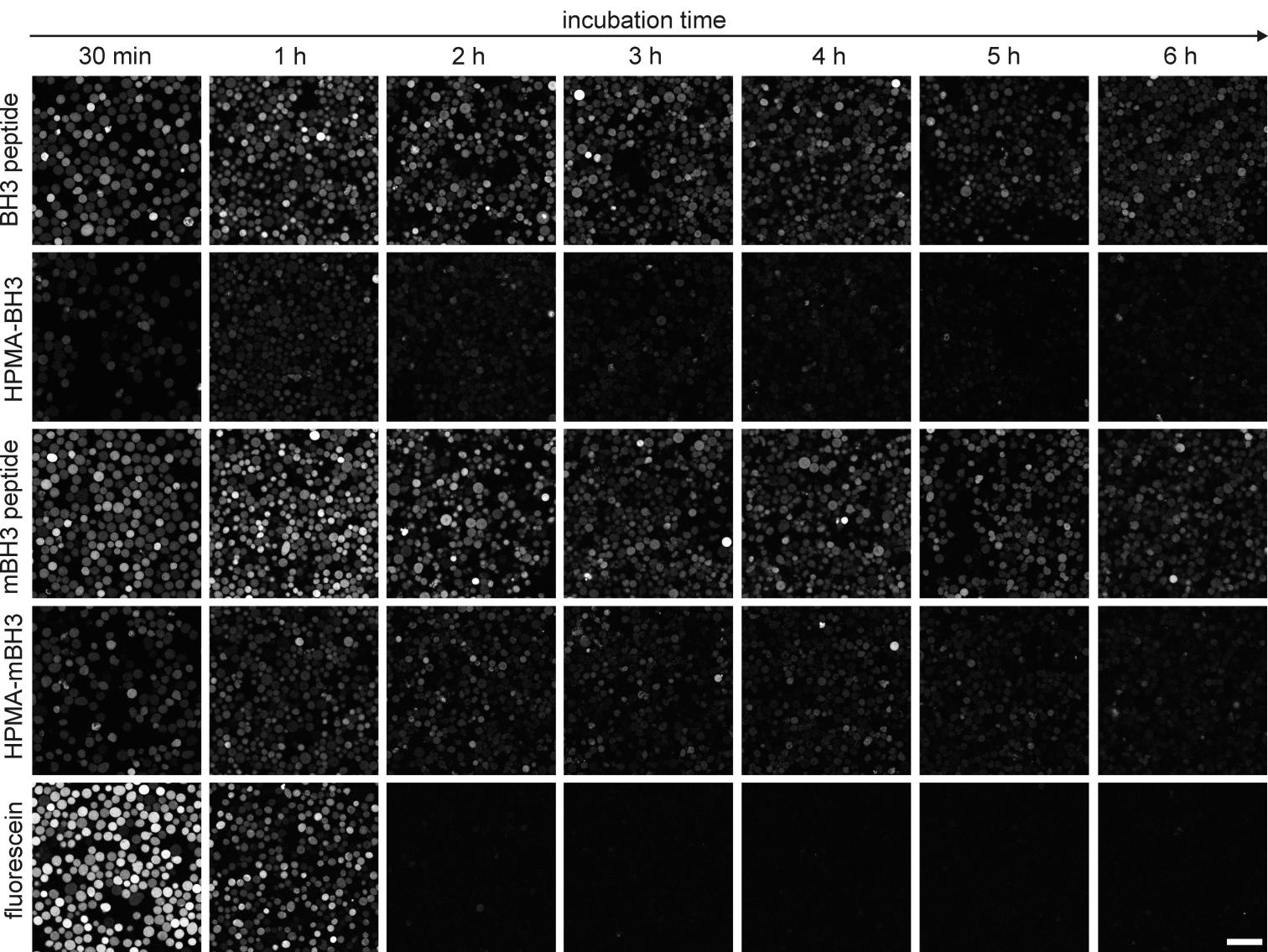


Figure 4

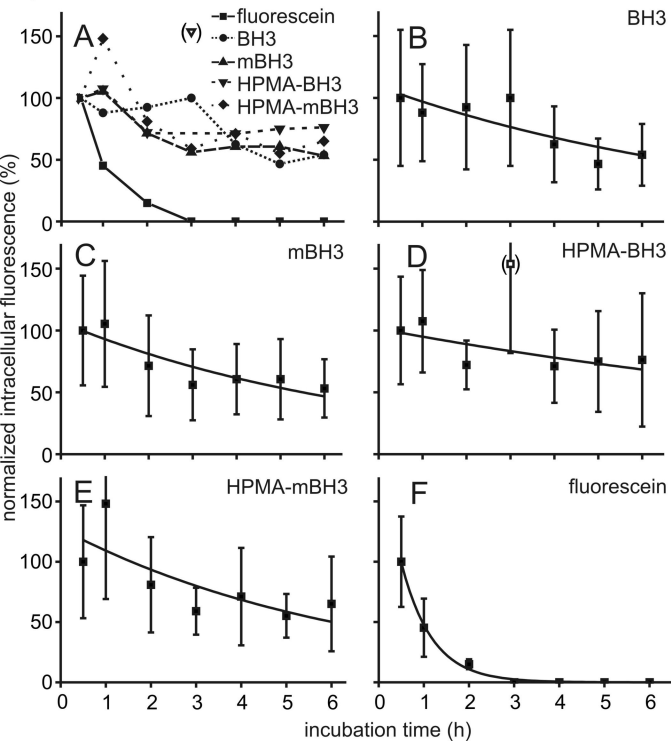


Figure 5

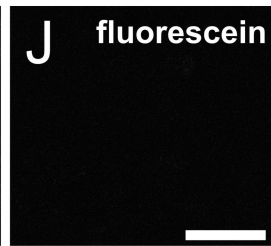
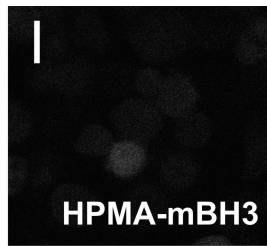
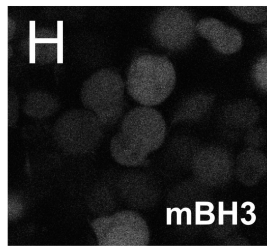
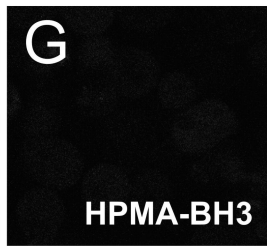
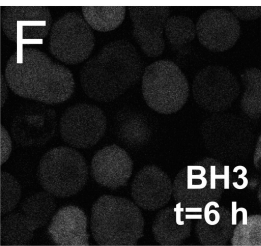
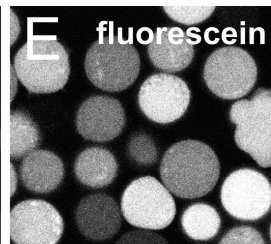
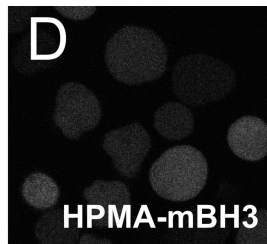
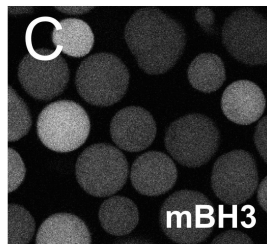
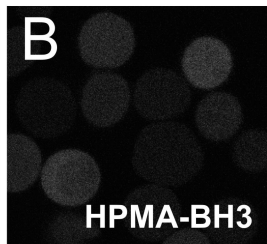
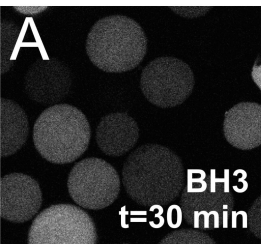


Figure 6

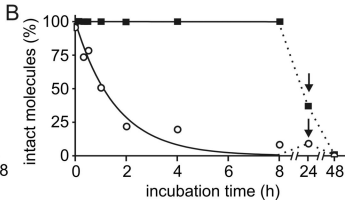
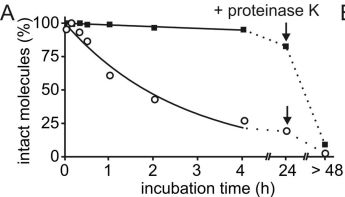


Figure 7

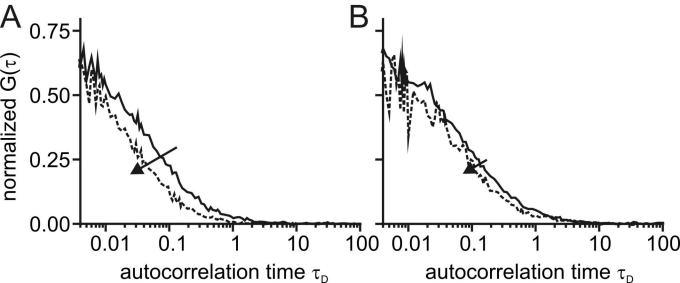


Figure 8

